U.S. DEPARTMENT OF COMMERCE
NATIONAL OCEANIC AND ATMOSPHERIC ADMINISTRATION
NATIONAL WEATHER SERVICE
OFFICE OF SYSTEMS DEVELOPMENT
TECHNIQUES DEVELOPMENT LABORATORY

TDL OFFICE NOTE 87-3

FORECASTING TEMPERATURE, DEW POINT, AND MAXIMUM TEMPERATURE USING THE LOCAL AFOS MOS PROGRAM (LAMP)

Michael W. Cammarata

July 1987

FORECASTING TEMPERATURE, DEW POINT, AND MAXIMUM TEMPERATURE USING THE LOCAL AFOS MOS PROGRAM (LAMP)

Michael W. Cammarata

1. INTRODUCTION

The Techniques Development Laboratory (TDL) has undertaken a project called the Local AFOS MOS Program (LAMP) (Glahn, 1980; Glahn and Unger, 1986). The purpose of LAMP is to provide a forecasting system which can be run on a local minicomputer to produce objective guidance for all weather elements routinely contained in public and aviation forecasts for the 1 to 20 h time range. Input to the LAMP forecast system will be the centrally issued MOS forecasts, local observations, the output from locally run numerical models, and eventually, radar and satellite data.

LAMP is intended to serve as an update to the centrally issued MOS guidance forecasts since information available subsequent to that used in producing the MOS forecasts can be utilized. The relationships between LFM model inputs (0000 GMT cycle), MOS, LAMP, and forecast valid periods are shown in Fig. 1. In using LAMP to prepare public and aviation forecasts, the forecaster can incorporate local observations as late as 0800 GMT or even 0900 GMT into the objective guidance. The centralized MOS guidance is based upon observations made 5 to 6 hours earlier and on a model initialized 8 to 9 hours earlier than the observations available for preparing the official forecast. Ultimately, the meteorologist will be able to initiate the LAMP system at any time, freeing objective short-range guidance from dependence upon the two upper-air observation times.

The numerical models used in LAMP consist of a sea level pressure (SLP) model (Unger, 1982), a moisture model based upon the SLYH model (Younkin et al., 1965), and a trajectory model called CLAM (Grayson and Bermowitz, 1974). The models are driven by a 500-mb height forecast from an operational NMC model and are initialized with an objective analysis of surface data. These models will be run locally on a minicomputer under the control of the forecast office. The output from these models will then be combined statistically with hourly observations and centralized MOS forecasts to produce updated MOS guidance forecasts.

In this paper, the development and testing of a LAMP system for forecasting hourly temperatures and dew points and maximum temperature for 103 stations in the central United States is described. Regression equations were developed for each of the 103 stations and for each hour out to 20 hours from the initial time of 0800 GMT. In order to test the utility of the LAMP numerical models, two sets of equations were developed; one including predictors from the local observation, centralized MOS forecasts, and LAMP numerical models, and the other based only upon predictors from the local observation and the centralized MOS forecasts. LAMP system forecasts from each of the equation sets were then included in a comparative verification along with MOS forecasts interpolated in space and time to conform with the stations and projections included in the LAMP system.

2. PREDICTANDS

The predictand data consisted of observations of temperature and dew point at each of the hours 1 through 20 after the initial time of 0800 GMT and the observed maximum temperature during this time period. The area of study, bounded roughly by 105° W long., 90° W long., 45° N lat., and 29° N lat., was selected to include the area planned by the National Weather Service for the Modernization and Restructuring Demonstration (MARD). Within this area, 103 stations were selected of which 63 were MOS stations and 40 were non-MOS stations. A listing of the stations included in this study is given in Appendix I. Four cool seasons (October through March) of data, beginning in October 1977 were used for equation development with a fifth cool season (October 1981-March 1982) reserved for independent verification.

3. POTENTIAL PREDICTORS

The potential predictors used in the development of hourly temperature and dew point forecast equations and those for maximum temperature forecast equations are listed in Tables 1 and 2 respectively. The predictor data pertained to the same time period as that previously described for the predictand data. The potential predictors come from three sources: (1) hourly surface observations (OBS), (2) centrally produced MOS forecasts, and (3) output from the SLP, SLYH, and CLAM models.

For temperature and dew point, the 0800 GMT observations were included in the predictor pool for all 20 forecast projections. MOS forecasts were obtained for non-MOS stations by using a weighted average of the forecasts from surrounding MOS stations. The MOS stations included in the weighted average for each non-MOS station were determined subjectively, based upon geographical and climatological considerations. Table 3 shows the stations and weights used to determine MOS forecasts for non-MOS stations. Centrally produced MOS forecasts of temperature and dew point from the 0000 GMT forecast cycle are valid at 3-h intervals beginning with 0600 GMT. Since hourly forecasts were to be made, a simple linear interpolation was used to produce MOS forecasts at intermediate hours. In this manner, the predictor pool for each projection contained MOS temperature and dew point forecasts valid for that projection. Similarly, the predictor pool for each projection contained LAMP numerical model forecast fields interpolated to the stations, valid at that projection.

The predictor pool for maximum temperature was essentially the same as that for temperature and dew point except that MOS maximum temperature forecasts were substituted for the MOS temperature and dew point forecasts. While no time interpolation was needed for the MOS maximum temperature forecasts, the space interpolation scheme was the same as that used for MOS hourly temperature and dew point forecasts. In addition, LAMP numerical model predictors valid at multiple projections were made available for selection.

4. EQUATION DEVELOPMENT

Since temperature and dew point forecast equations were needed for each of 20 projections, forecast consistency between predictands and in time was a major concern. Forecast consistency in space was also an important consideration since equations were to be developed for 103 stations from the same general geographic region. One way to ensure forecast consistency between

related predictands and in space and time is to include the same predictors in the equations for all stations, predictands, and projections. To this end, a screening regression program was used to develop single station equations for temperature and dew point for all 20 projections and all 103 stations simultaneously. Similarly, single station equations were developed simultaneously for maximum temperature at all 103 stations.

A forward stepwise screening proceedure was used for predictor selection in which the first predictor selected is that which yields the largest reduction of variance (RV) for any combination of station, predictand, and projection. The second predictor selected is that predictor which, together with the first predictor, yields the greatest RV for any combination of station, predictand, and projection. The selection process continues in this manner as long as the additional RV contributed by the next predictor is $\geq$ 0.5% or until 12 predictors have been selected. The limit of 12 predictors was imposed because this number of predictors has been found to be about optimum for MOS regression equations (Annett et al., 1972; Bocchieri and Glahn, 1972). While this limitation may appear restrictive for equations which are derived simultaneously in the manner described above, initial experimentation suggested that beyond 10 to 12 predictors, the additional RV achieved through further predictor selection is insignificant.

For purposes of evaluation, three sets of forecasts were generated and included in a comparative verification. The first set of forecasts was simply taken to be the MOS forecasts interpolated in space and time as described previously (hereafter referred to as M for MOS). The second set of forecasts were generated with equations developed from a predictor pool limited to the space and time interpolated MOS forecasts and the 0800 GMT observation (hereafter referred to as MO for MOS + Obsevations). The third set of forecasts were generated with equations developed from the entire predictor pool consisting of space and time interpolated MOS forecasts, the 0800 GMT observations, and the numerical model fields (hereafter referred to as MOM for MOS + Observations + Models).

Tables 4 and 5, respectively, show the predictors included in the MOM and MO forecast equations for hourly temperature and dew point. Similarly, Tables 6 and 7, respectively, show the predictors included in the MOM and MO forecast equations for maximum temperature. The predictors are listed in the order chosen by the screening regression program, and the additional RV provided by each predictor for the listed combination of station, predictand, and projection is also shown.

As might be expected, the most important predictors selected for both the MOM and MO temperature and dew point equations were the observed temperature and dew point at initial time and MOS forecasts of temperature and dew point. The most important numerical model predictors selected for the MOM equations were the 1-h saturation deficit and the 500-1000 mb thickness.

For the maximum temperature equations, MOS maximum temperature was the most important predictor selected for both the MOM and MO equations, accounting for a RV of over 0.95. For both the MOM and MO equations, no other predictor accounted for an additional RV of over 0.05 for any station.

5. RESULTS AND EVALUATION

The equations derived as described in Section 4 were used to make forecasts of hourly temperature, dew point, and maximum temperature for the period 1 October 1981-30 March 1982. Forecasts were made for each of the 103 stations in the sample and were matched with corresponding surface observations for the purpose of verification. MOS and non-MOS stations were verified separately. However, the data from all stations within each of the two groups were combined after being further segregated by predictand and forecast projection.

For MOS stations, the number of cases totaled about 9,000 for hourly temperature and dew point and about 8,500 for maximum temperature. For non-MOS stations, the number of cases was about 3,400 for hourly temperature and dew point and about 3,000 for maximum temperature.

In interpreting the verification results presented here, it is important to keep in mind the relationship between the true MOS projection based upon the 0000 GMT forecast cycle and the corresponding LAMP projection based upon a 0800 GMT initial time. The MOS forecasts used in this study are based upon the 0000 GMT LFM and use observations from 0300 GMT. So, a 1-h projection for MOM and MO is really a 6-h projection for M. In operations, the MOS guidance frequently uses the 0200 GMT observation, in which case a 1-h projection for MOM and MO would be a 7-h projection for M.

The mean absolute error (MAE) and bias were used to assess the average performance of the forecasting systems. In addition, histograms of forecast errors were constructed to determine the extent to which large forecast errors occurred. Finally, a few selected cases were analyzed to evaluate the performance of the forecasting systems during specific synoptic conditions.

A. Hourly Temperatures--MOS Stations

Figure 2 shows that the MOM and MO forecasts have virtually the same MAE at all projections for MOS stations. This indicates that the LAMP numerical model predictors contain little predictive information in addition to that which is contained in the M forecast and the initial observation.

MOM and MO produce significantly better forecasts than M out to about 7 hours from initial time; however, the magnitude of the improvement over M decreases steadily with time during this period. This improvement over M in the early projections is attributable to the information contained in the initial observations. After the 7-h projection, MOM and MO show little improvement over M with the greatest improvements at non-standard MOS projections, i.e., projections for which a time interpolation has been performed. The linear interpolation of MOS forecasts at 3-h intervals to 1-h projections results in relatively large MAE's at non-standard MOS projections, especially near the mean times of minimum and maximum temperature (projections 5-6 and 14-15, respectively). An examination of M forecast biases (Fig. 3) and a comparison of the mean M forecast and mean observed temperature curves (Fig. 4) illustrates that the larger forecast errors at non-MOS projections is the result of attempting to approximate a non-linear phenomena (the daily temperature curve) with a linear interpolation. The biases for MOM and MO are near zero for all projections; thus it appears that the regression analysis used in the development of MOM and MO effectively compensates for this problem.

B. Hourly Temperatures - non-MOS Stations

Figure 5 indicates that MOM produces slightly better forecasts than MO at most projections for non-MOS stations. Both MOM and MO are substantially better than M at all projections with the largest improvements occurring before 7 hours.

The relatively poor performance of M at non-MOS stations is attributable to the space interpolation of nearby MOS forecasts to non-MOS stations. This procedure entirely neglects important local effects. The extent to which the regression analysis calibrates for errors introduced by the space interpolation is shown in Figures. 6-8. Note that M forecasts at MOS stations are far superior to those at non-MOS stations at all projections whereas MOM and MO forecasts at MOS stations are only marginally better than those at non-MOS stations.

Figure 9a shows that M forecasts at non-MOS stations exhibit a strong warm bias relative to forecasts at MOS stations. This relative warm bias is also apparent to a much lesser extent in the MOM and MO forecasts (Figs. 9b and 9c) and only for projections after about 7 hours. It is noteworthy that this relative warm bias is absent in the early projections of the MOM and MO forecasts. This is a reflection of the predictive information contained in the initial observation.

C. Hourly Temperatures--Distribution of Forecast Errors

Histograms of MOM forecast errors were constructed for each projection and for both MOS and non-MOS stations (not shown). All distributions were approximately normal in appearance and tended to exhibit a larger variance with increasing projection out to around the 10-h projection. After the 10-h projection, all distributions were quite similar in appearance. The distributions for non-MOS stations were similar to those for MOS stations.

In order to compress the information contained in the distributions of forecast errors, graphs were constructed indicating the percentage of forecast errors falling within $\pm$ 10°F, $\pm$ 5°F, $\pm$ 3°F, and $\pm$ 1°F of the observed temperature. These graphs are shown in Fig. 10 for MOS stations and Fig. 11 for non-MOS stations.

The percentage of forecast errors falling within each of the stated limits is virtually identical for MOM and MO at all projections and for both MOS and non-MOS stations. For MOS stations, the percentage of forecast errors falling within $\pm$ 10°F is nearly the same for all forecast models at all projections. The percentage of forecast errors falling within $\pm$ 5°F, $\pm$ 3°F, and $\pm$ 1°F for MOM and MO are significantly higher than for M out to about the 7-h projection, after which, the improvement over M is small except near the average time of maximum temperature (projections 14 and 15). For non-MOS stations, MOM and MO produce results superior to those of M at all projections and for all thresholds with the largest improvements occurring for projections 1-7.

D. Hourly Temperatures--Case Studies

In order to gain an understanding of how the forecasting models perform in specific synoptic conditions, several case studies were examined. Case studies were limited to situations involving the passage of one or more sharp frontal boundries in a short period of time, resulting in rapid and relatively large changes in temperature. It is hoped that the LAMP forecasting system will be able to resolve such changes with a fair degree of accuracy.

The results of the case studies were not consistent so that conclusions could not be made as to which of the LAMP forecasting systems (MOM or MO) performed better. However, the case studies did lead to the following general conclusions:

1) The initial observation strongly influences MOM and MO during the early projections. If the initial observation differs significantly from the MOS forecast (and consequently the M forecast) valid at that time, MOM and MO will also differ significantly from MOS (and M) with the magnitude of this difference decreasing with increasing projection.

2) In the later projections, MOM and MO are strongly dependent upon MOS. If the LFM and consequently MOS are in error, MOM and MO will in most cases exhibit similar errors.

E. Hourly Dew points

Figures 12-18 for hourly dew point correspond to Figures 2, 5, 6, 7, 8, 10, and 11 for hourly temperature. The conclusions regarding hourly dew point are basically the same as those for hourly temperature and will not be repeated here in detail except for the following items which are worthy of mention:

1) The initial observation appears to have a somewhat greater memory for dew point than for temperature. This is evidenced in the lower initial MAE for MOM and MO and the longer decay time for the improvement of MOM and MO over M. The improvement of MOM and MO over M extends out to projection 9 (versus projection 7 for temperature) for MOS stations and is evident at all projections for non-MOS stations but becomes nearly constant at about projection 9 or 10 (versus projection 7 or 8 for temperature).

2) The MAE curves for hourly dew point, especially for M, exhibit less variability than those for hourly temperature. This is because the mean daily observed dew point curve (not shown) has a much smaller diurnal range and is more linear than the corresponding curve for hourly temperature.

3) The difference in MAE between MOS and non-MOS stations is slightly larger for dew point than for temperature for all models, most notably for projections 9-15.

F. Maximum Temperature

An examination of Fig. 19 shows that for MOS stations, M, MOM, and MO have virtually the same MAE. At non-MOS stations, both MOM and MO clearly outperform M with MOM performing slightly better than MO. Even so, the difference between MOM and MO forecasts is 1°F or less nearly 70% of the time and within 3°F almost 95% of the time.

6. SUMMARY AND CONCLUSIONS

Experimental LAMP hourly temperature, hourly dew point, and maximum temperature equations were developed and tested for 103 stations in and around the MARD area. Four cool seasons of data were used for the purpose of equation development and one cool season of data for independent verification.

Two sets of equations were developed through the use of a screening regression program. The predictors for the first set of equations (MO) included space and time interpolated MOS forecasts and the initial surface observation. Additional predictors consisting of the output from the LAMP SLP, SLYH, and CLAM advective models were made available for the second set of equations (MOM).

Forecasts generated from the two sets of LAMP equations along with space and time interpolated MOS forecasts were included in a comparative verification. For purposes of verification, MOS and non-MOS stations were treated separately. The major conlusions arising from this study are as follows:

A Hourly Temperature and Dew point

1) The greatest potential benefit in using MOM and MO appears to occur at non-MOS stations where the simple linear space interpolation of nearby MOS forecasts is reflected in the poor performance of M. The regression analysis used in the development of MOM and MO appear to effectively calibrate for the errors in M resulting from the space and time interpolations.

2) MOM and MO forecasts are strongly dependent upon the initial surface observations during the early projections. As a result, MOM and MO forecasts significantly improve upon M out to about the 7-h projection for both MOS and non-MOS stations. The magnitude of this improvement decreases with increasing projection, reflecting the diminishing utility of the initial observation with time.

3) The linear interpolation of MOS forecasts at 3-h intervals to 1-h projections results in relatively large MAE's for M at non-standard MOS projections, especially near the average time of maximum and minimum temperature.

4) The MOM and MO forecasts are largely dependent upon the MOS forecast in later projections. If the MOS forecasts for the later projections are in error, MOM and MO will in general exhibit similar errors.

5) For MOS stations, the LAMP numerical models add little if any predictive information in addition to that which is already contained in the MO forecast. The LAMP models, however, appear to contribute some useful information for non-MOS stations where MOM produces slightly better forecasts than MO at most projections. The LAMP numerical models appear to have their greatest impact in terms of forecast differences between MOM and MO for projections 10-15.

B Maximum Temperature

1) For MOS stations, there appears to be no strong advantage to using MOM or MO over M as each of these predictive schemes appears to perform equally as well. For non-MOS stations however, MOM and MO clearly outperform M with MOM performing slightly better than MO.

REFERENCES

Annett, J. R., H. R. Glahn, and D. A. Lowry, 1972: The use of Model Output Statistics (MOS) to estimate daily maximum temperatures. NOAA Technical Memorandum NWS-45, National Oceanic and Atmospheric Administration, U.S. Department of Commerce, 14 pp.

Bocchieri, J. R., and H. R. Glahn, 1972: The use of Model Output Statistics for predicting ceiling height. Mon. Wea. Rev., 100, 869-879.

Glahn, H. R., 1980: Plans for the development of a local AFOS MOS program (LAMP). Preprints Eighth Conference on Weather Forecasting and Analysis, Denver, Amer. Meteor. Soc., 302-305.

_____, and D. A. Unger, 1986: A local AFOS MOS program (LAMP) and its application to wind forecasting. Mon. Wea. Rev., 114, 1313-1329.

Grayson, T. H., and R. J. Bermowitz, 1974: A subsynoptic update model with application to aviation weather. Report No. FAA-RD-74-100, Techniques Development Laboratory, National Weather Service, NOAA, U. S. Department of Commerce, 48 pp.

Unger, D. A., 1982: The sea level pressure prediction model of the local AFOS MOS program. NOAA Technical Memorandum NWS TDL-70, National Oceanic and Atmospheric Administration, U. S. Department of Commerce, 33 pp.

Younkin, R. J., J. A. LaRue and F. Sanders, 1965: The objective prediction of clouds and precipitation using vertically integrated moisture and adiabatic vertical motions. J. Appl. Meteor., 4, 3-17.

Table 1. Potential predictors available to the screening regression program for the development of LAMP temperature and dew point equations. Observed variables have values for initial time only (0800 GMT), while MOS and model variables have values at each projection.

Variable	Source
Temperature	MOS
Dew Point	MOS
Temperature	Observation
Dew Point	Observation
U Wind	Observation
V Wind	Observation
Sky Cover	Observation
1000-500 mb Thickness	SLP Model
1-h Saturation Deficit	SLYH Model
1000-mb Height	SLP Model
Ceiling Height	CLAM Model
Visibility	CLAM Model
Sky Cover	CLAM Model
1000-mb Geostrophic U Wind	SLP Model
1000-mb Geostrophic V Wind	SLP Model

Table 2. Potential predictors made available to the screening regression program for the development of LAMP maximum temperature equations.

Variable	Projection																	
	0	1	2	3	4	5	6	7	8	9	10	11	12	13	14	15	16	17	18
MOS MAX Temperature																	x		
Observed Temperature	x																		
Observed dew point	x																		
Observed U Wind	x																		
Observed V Wind	x																		
Observed Sky Cover	x																		
Model 5-10 Thickness									x		x		x		x		x		
Model 1-h Sat Deficit									x		x		x		x		x		
Model 1000-mb Height									x		x		x		x		x		
Model Ceiling Height										x			x			x			
Model Visibility										x			x			x			
Model Sky Cover										x			x			x			
Model 1000-mb Geo U Wind										x			x			x			
Model 1000-mb Geo V Wind										x			x			x			

Table 3. Non-MOS stations with the weighting formulation used to determine the MOS forecast. For example, the MOS temperature forecast for CNM would be determined be adding the MOS temperature forecast for ROW to 3 times the MOS temperature forecast for MAF and dividing by 4.

Non-MOS Station	Weighting Formulation
AKO	DEN,GLD
ATY	HON,ABR
CDS	AMA,LBB
CGI	JBR,EVV,STL
CID	MLI,ALO,DSM
CNM	ROW,3*MAF
CNU	TOP,ICT,TUL
CVS	TCC,ROW,2*LBB
DAL	DFW
DHT	TCC,3*AMA
DMN	4*ELP,TUS
DUG	3*TUS,ELP
EGE	GJT
ELD	TXK,SHV,2*JAN
FYV	FSM,2*SGF
GAG	2*DDC,AMA
GCK	DDC,GLD
GGG	SHV,DFW,LFK
GUP	ABQ,SOW
HMN	ABQ,ELP,ROW
HRO	2*SGF,FSM
INK	ROW,4*MAF
JLN	SGF,TUL
LAR	3*CPR,CYS
LHX	2*COS,GLD
LVS	ABQ,4*TCC
MLU	3*SHV,TXK,JAN
NBE	DFW
NQA	MEM
OTM	DSM,BRL
PNC	ICT,TUL
RWF	FSD,MSP
RWL	3*RKS,CPR
SLN	RSL,CNK,ICT,TOP
SPS	OKC,DFW
TAD	TCC,4*COS
TYR	DFW,SHV
UIN	BRL,SPI,COU
VIH	SGF,COU,STL
WRL	LND,SHR

Table 4. Predictors included in the MOM temperature and dew point equations. The additional RV afforded by each predictor and the station, projection, and predictand to which it corresponds are also shown.

Predictor	RV	Station	Predictand	Projection
Observed Dew Point	0.995	PIA	DWPT	1
MOS Temperature	0.862	DMN	TEMT	16
MOS Dew Point	0.262	MAF	DWPT	16
Observed Temperature	0.189	CNM	TEMP	1
Model 1-h Saturation Deficit	0.076	LVS	DWPT	14
Model 1000-500 mb Thickness	0.051	TAD	DWPT	15
Model 1000-mb Geostrophic U Wind	0.041	BFF	DWPT	12
Model 1000-mb Height	0.038	TAD	DWPT	11
Model Ceiling Height	0.018	TYR	TEMP	12
Model 1000-mb Geostrophic V Wind	0.015	LAR	TEMP	20
Observed U Wind	0.013	LAR	DWPT	18
Observed V Wind	0.012	BFF	DWPT	15

Table 5. Same as Table 4 except for MO equations.

Predictor	RV	Station	Predictand	Projection
Observed Dew Point	0.995	PIA	DWPT	1
MOS Temperature	0.862	DMN	TEMP	16
MOS Dew Point	0.262	MAF	DWPT	16
Observed Temperature	0.189	CNM	TEMP	1
Observed Sky Cover	0.023	GUP	TEMP	19
Observed U Wind	0.020	ELD	DWPT	9
Observed V Wind	0.015	EGE	DWPT	13

Table 6. Predictors included in the MOM maximum temperature equations. The predictor projections for the LAMP numerical model predictors are in hours from the LAMP initial time of 0800 GMT. The additional RV afforded by each predictor and the call letters of the station to which it corresponds are also shown.

Predictor		RV	Station
MOS Maximum Temperature		0.958	EAU
Model 1000-500 mb Thickness	16 h	0.046	GUP
Model 1000-mb Height	10 h	0.020	LVS
Observed Temperature		0.019	WRL
Model Ceiling Height	12 h	0.017	ELD
Model 1000-mb Geostrophic U Wind	8 h	0.016	MAF
Model 1000-mb Geostrophic V Wind	8 h	0.009	LVS
Observed Sky Cover		0.008	LAR
Model 1000-mb Geostrophic U Wind	16 h	0.007	TAD

Table 7. Predictors included in the MO maximum temperature equations. The additional RV afforded by each predictor and the call letters of the station to which it corresponds are also shown

Predictor	RV	Station
MOS Maximum Temperature	0.958	EAU
Observed Temperature	0.026	LAR
Observed Sky Cover	0.019	GUP
Observed V Wind	0.008	MAF

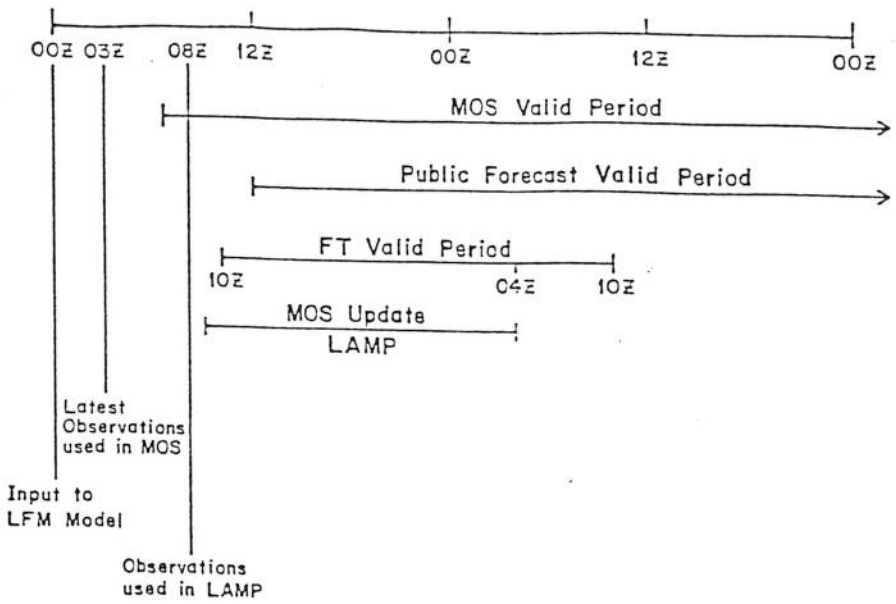

Figure 1. Relationship between inputs to the LFM model, MOS, and LAMP and the valid periods for the early morning forecasts assuming an FT issuance time of about 0900 GMT.

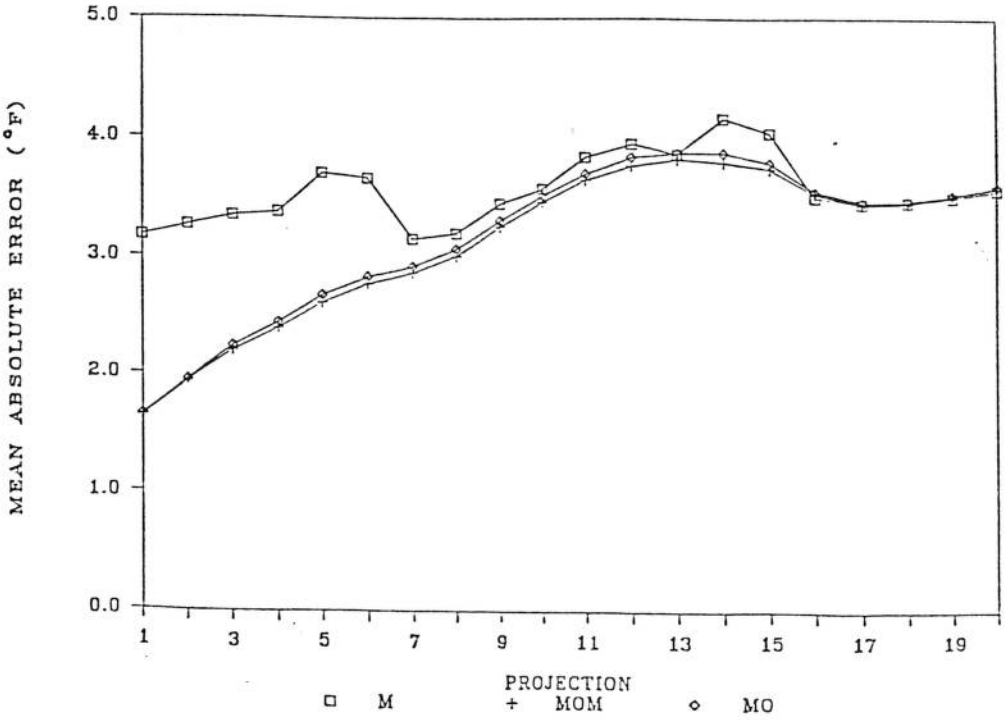

Figure 2. Mean absolute error vs. projection of MOM, MO, and M hourly temperature forecasts (MOS stations only).

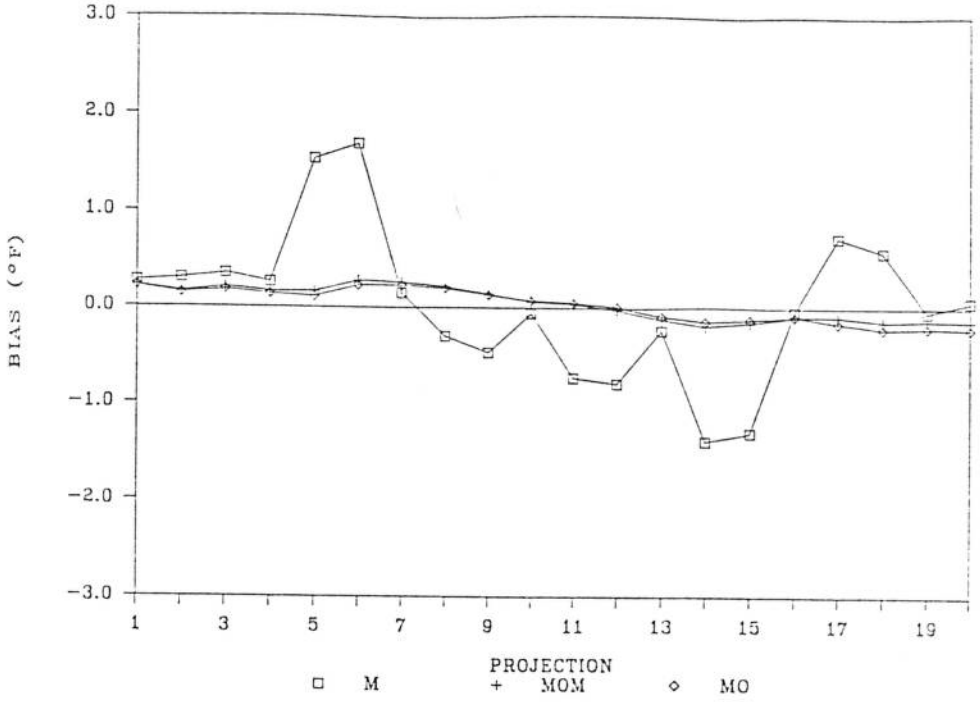

Figure 3. Bias vs. projection of MOM, MO, and M hourly temperature forecasts (MOS stations only).

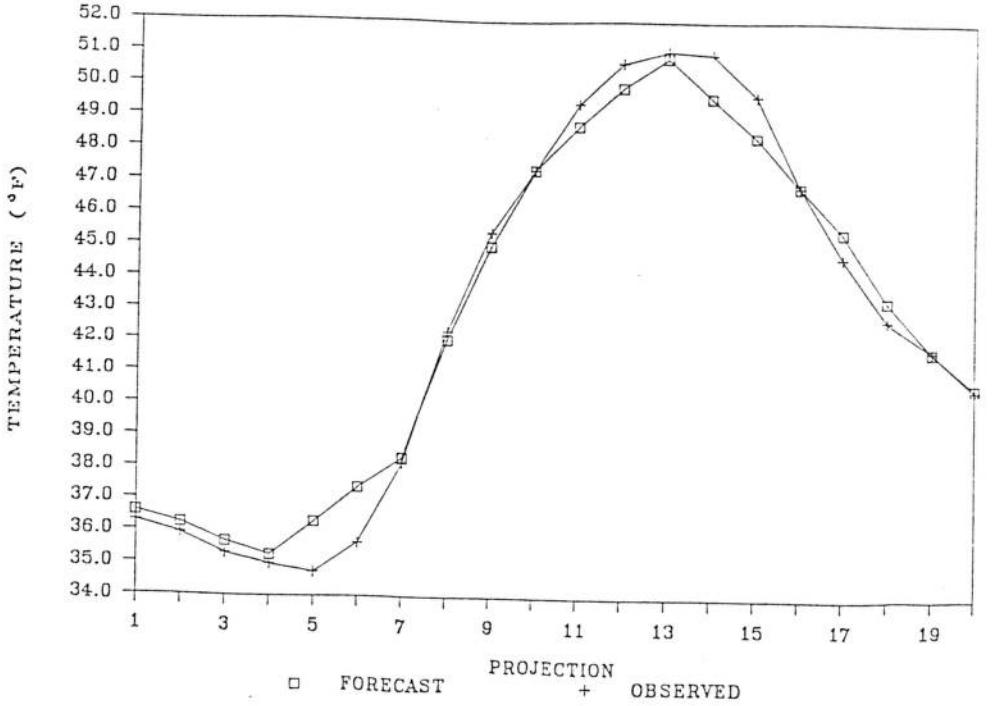

Figure 4. Mean space and time interpolated MOS forecast and observed temperature vs. projection (averaged over all stations).

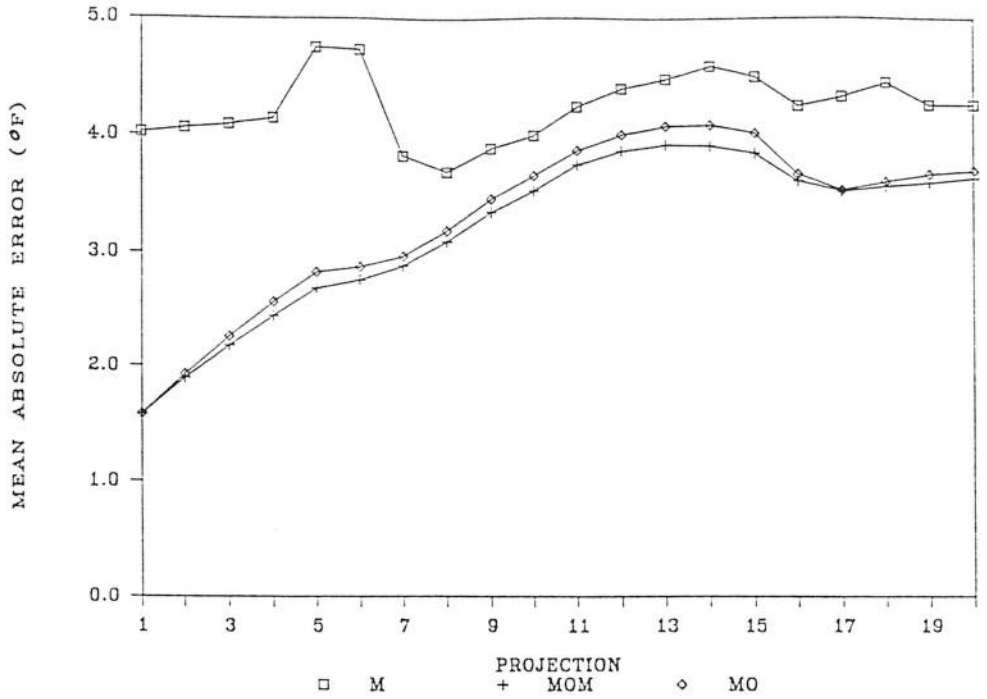

Figure 5. Mean absolute error vs. projection of MOM, MO, and M hourly temperature forecasts (non-MOS stations only).

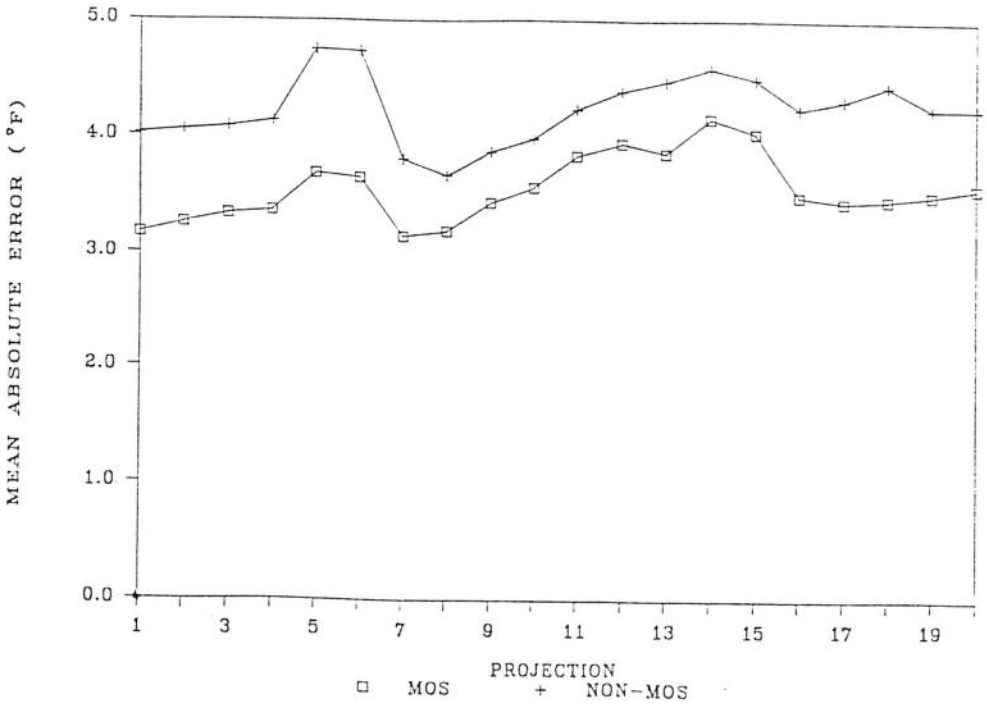

Figure 6. Mean absolute error vs. projection of M hourly temperature forecasts (MOS vs. non-MOS stations).

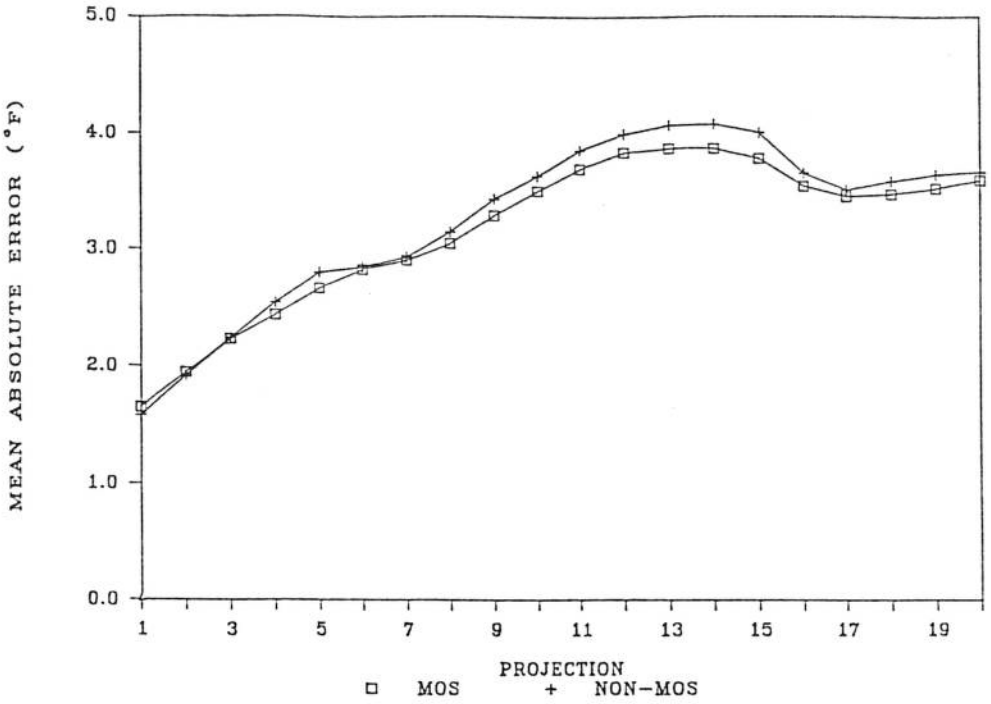

Figure 7. Mean absolute error vs. projection of MO hourly temperature forecasts (MOS vs. non-MOS stations).

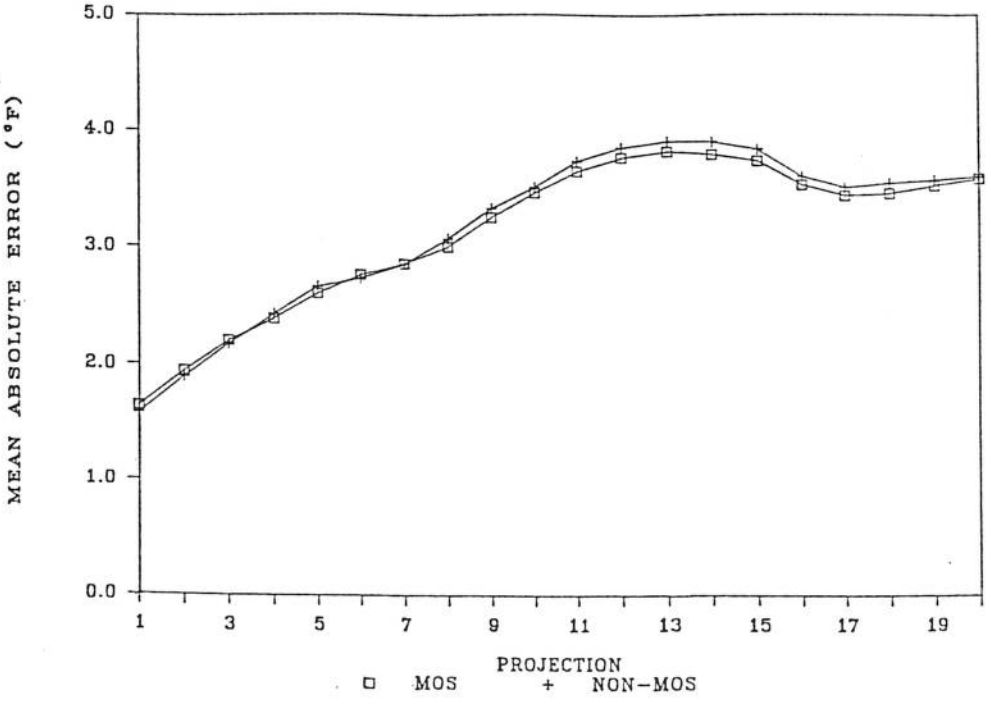

Figure 8. Mean absolute error vs. projection of MOM hourly temperature forecasts (MOS vs. non-MOS stations).

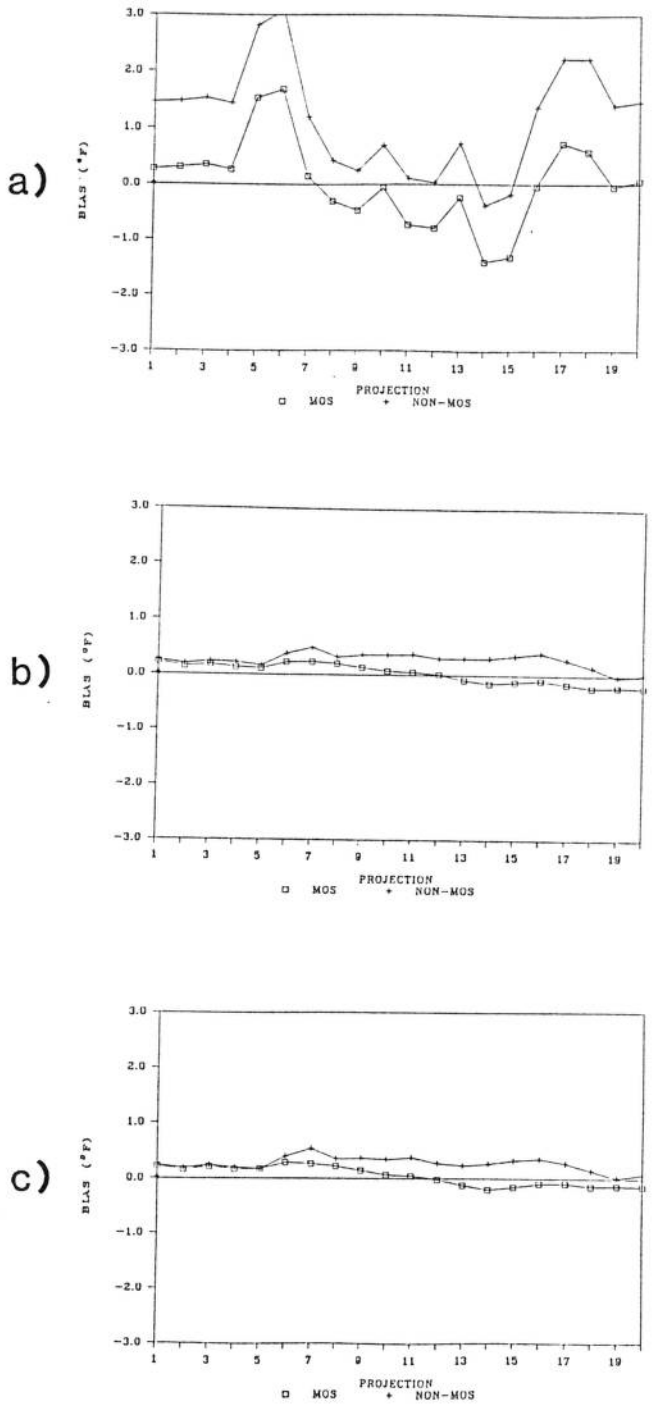

Figure 9. Bias vs. projection of hourly temperature forecasts (MOS vs. non-MOS stations): a) M forecasts, b) MO forecasts, and c) MOM forecasts.

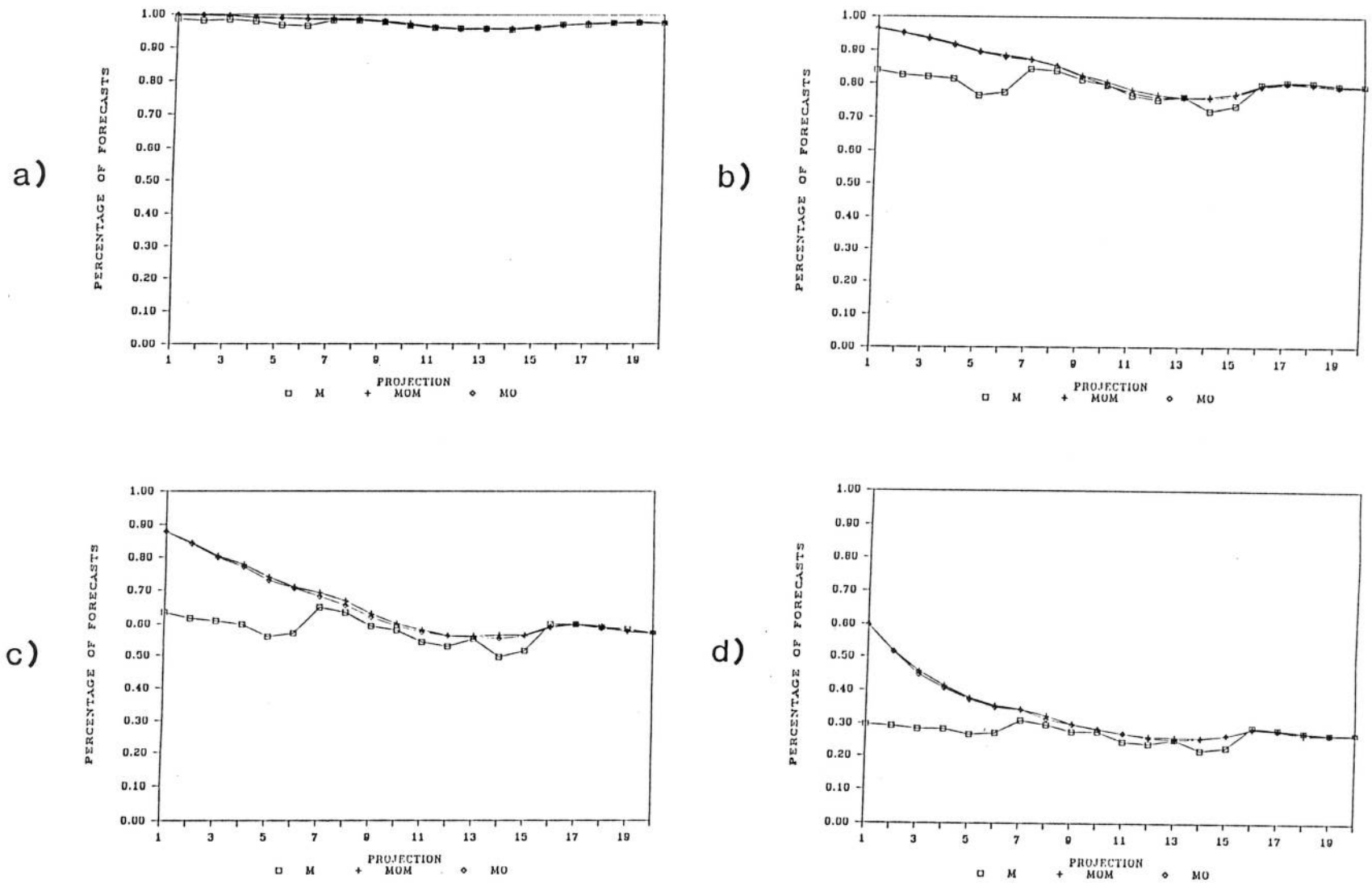

Figure 10. Percentage of hourly temperature forecasts within a) ±10°F, b) ±5°F, c) ±3°F, and d) ±1°F of the observed temperature by projection for M, MO, and MOM (MOS stations only).

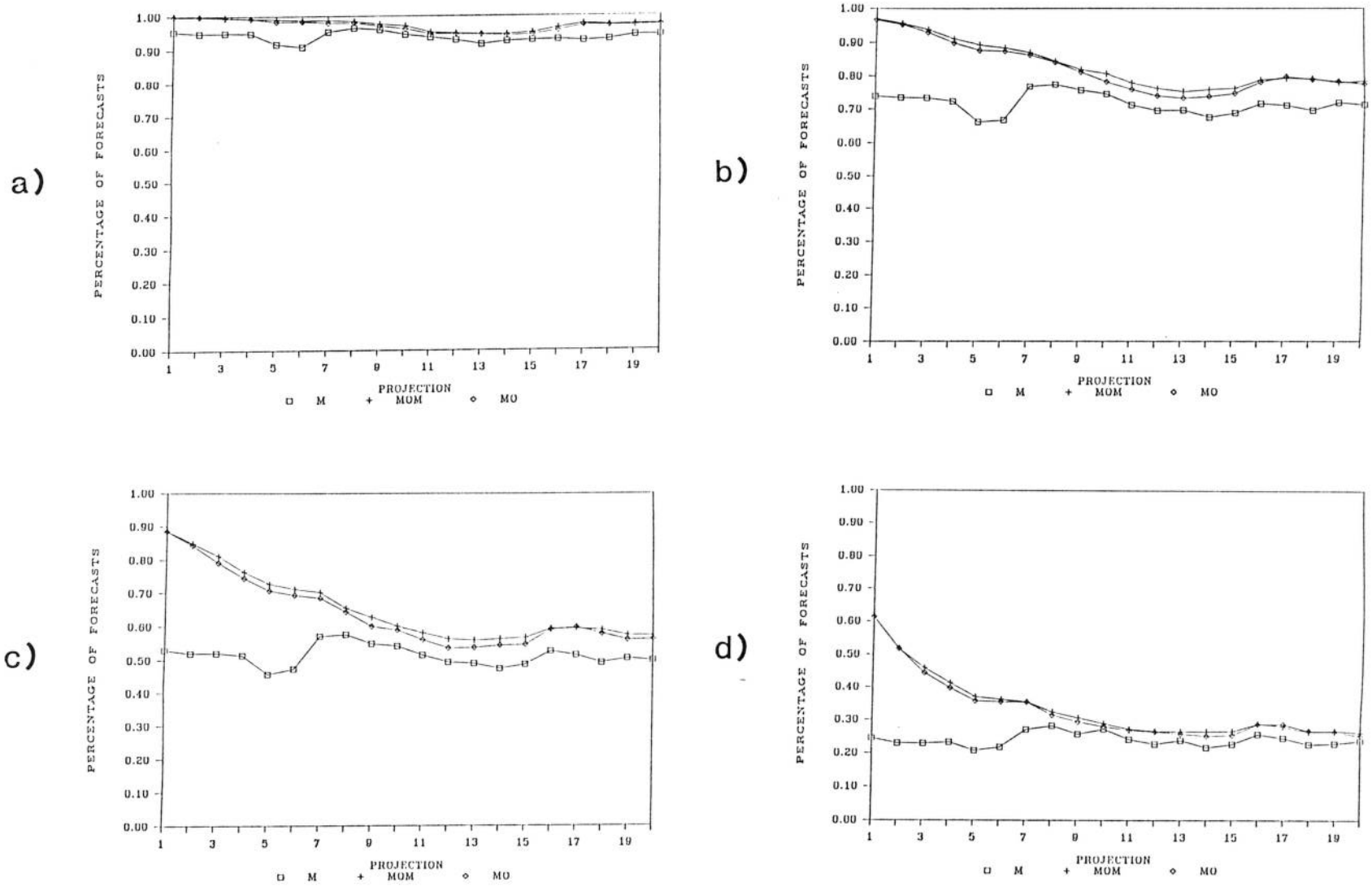

Figure 11. Same as Figure 10 but for non-MOS stations.

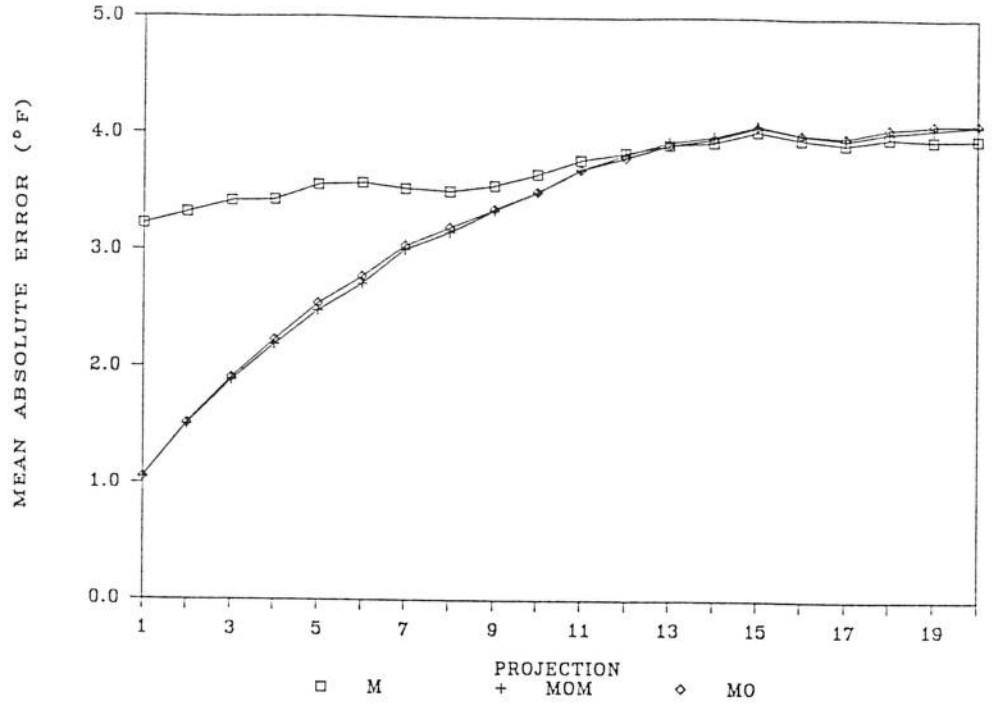

Figure 12. Mean absolute error vs. projection of M, MOM, and MO hourly dew point forecasts (MOS stations only).

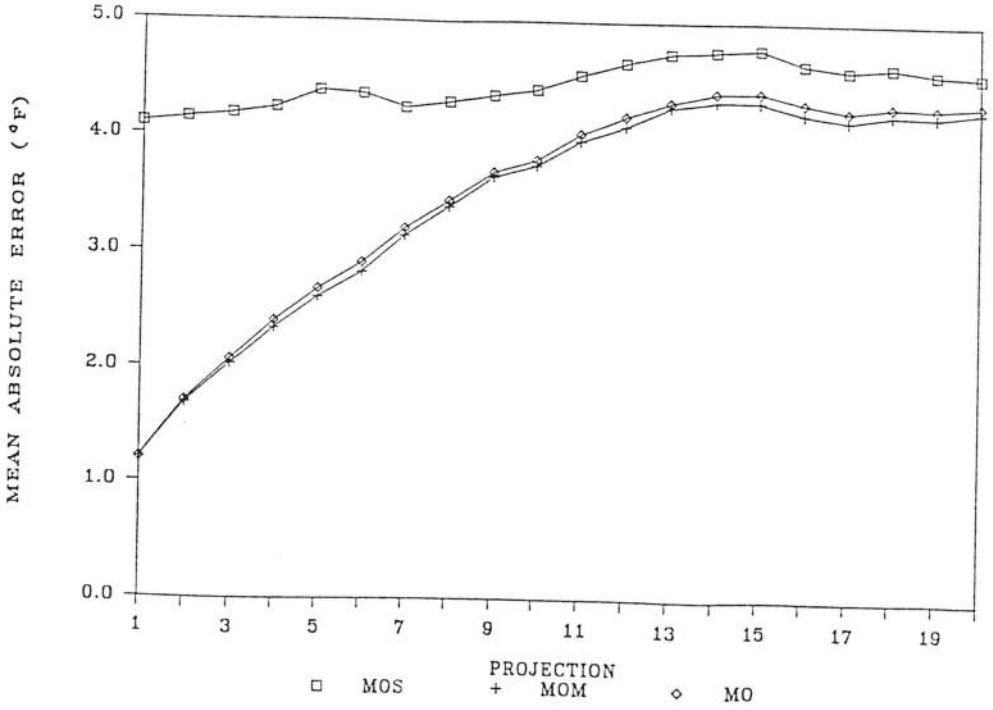

Figure 13. Mean absolute error vs. projection of M, MOM, and MO hourly dew point forecasts (non-MOS stations only).

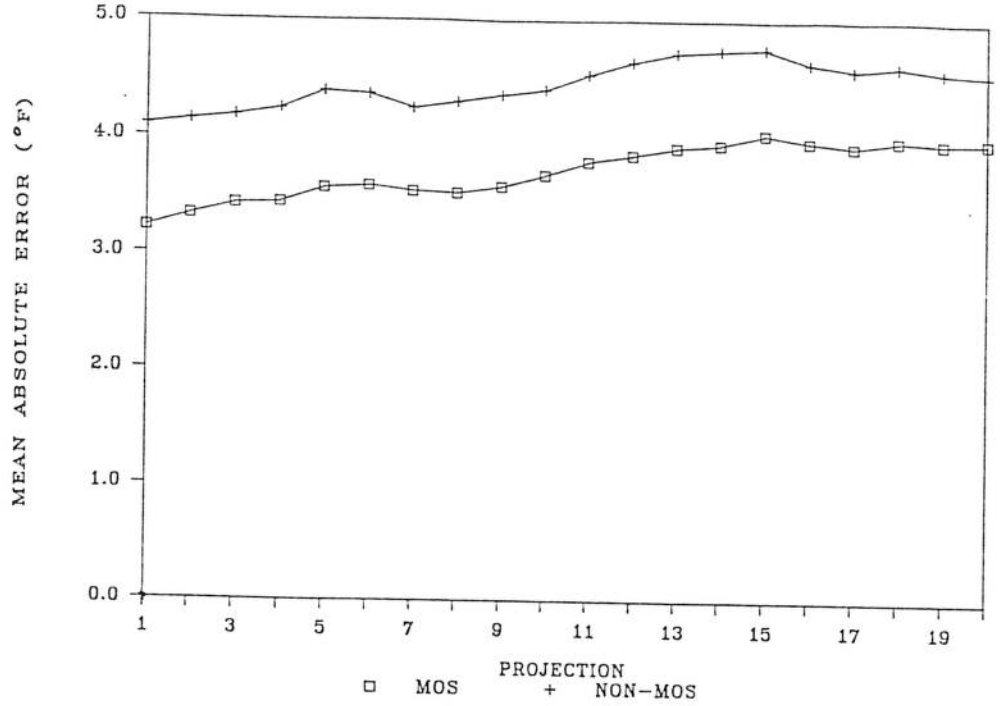

Figure 14. Mean absolute error vs. projection of M hourly dew point forecasts (MOS vs. non-MOS stations).

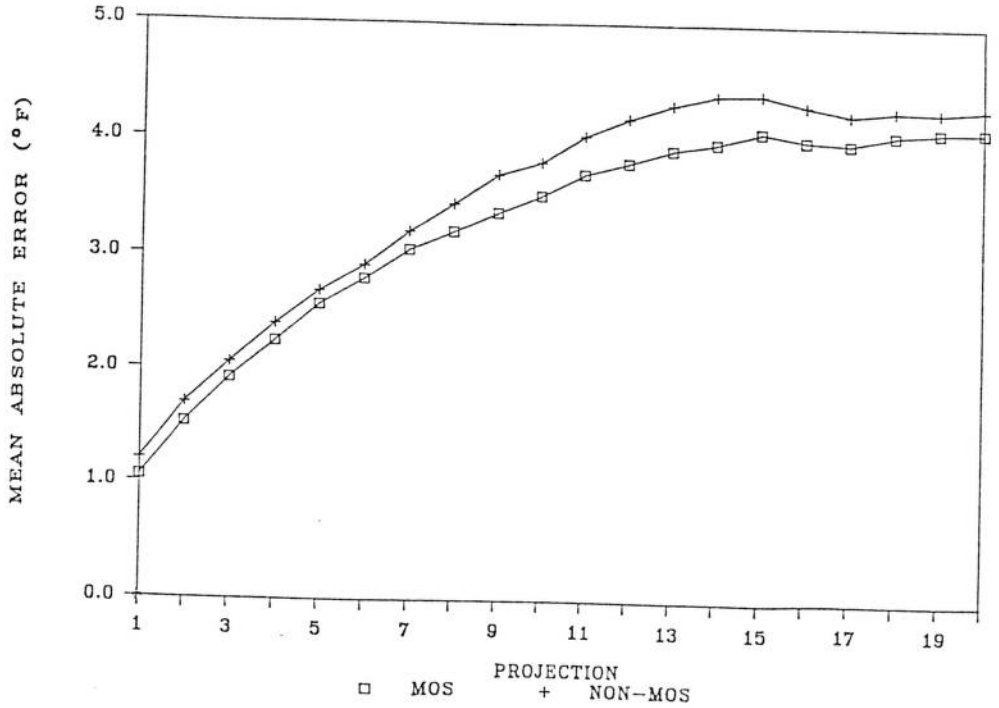

Figure 15. Mean absolute error vs. projection of MO hourly dew point forecasts (MOS vs. non-MOS stations).

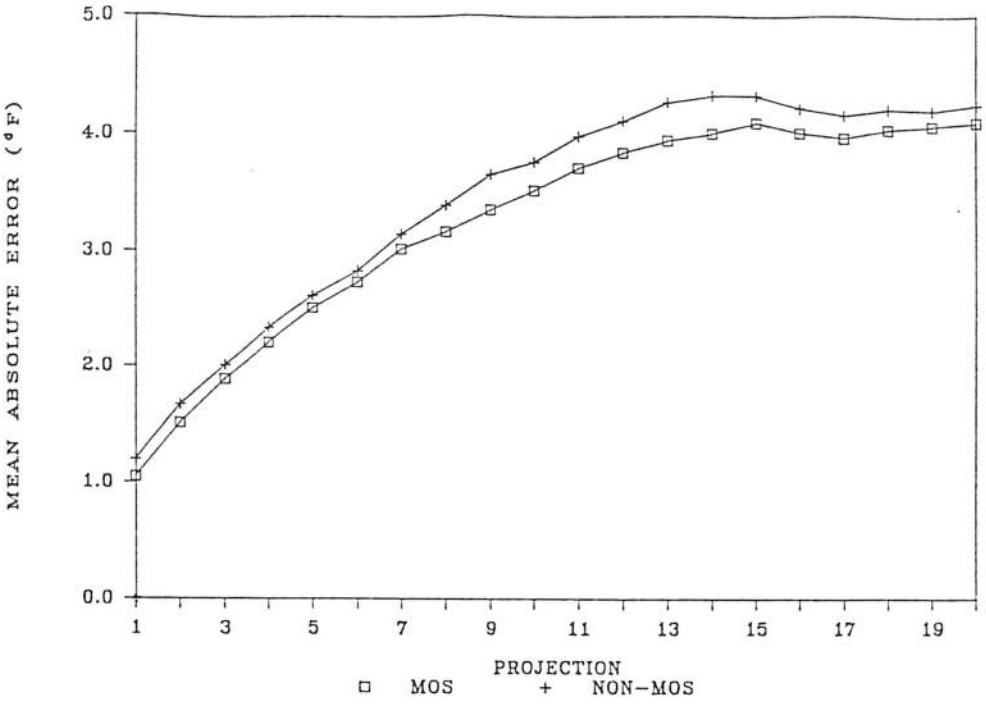

Figure 16. Mean absolute error vs. projection of MOM hourly dew point forecasts (MOS vs. non-MOS stations).

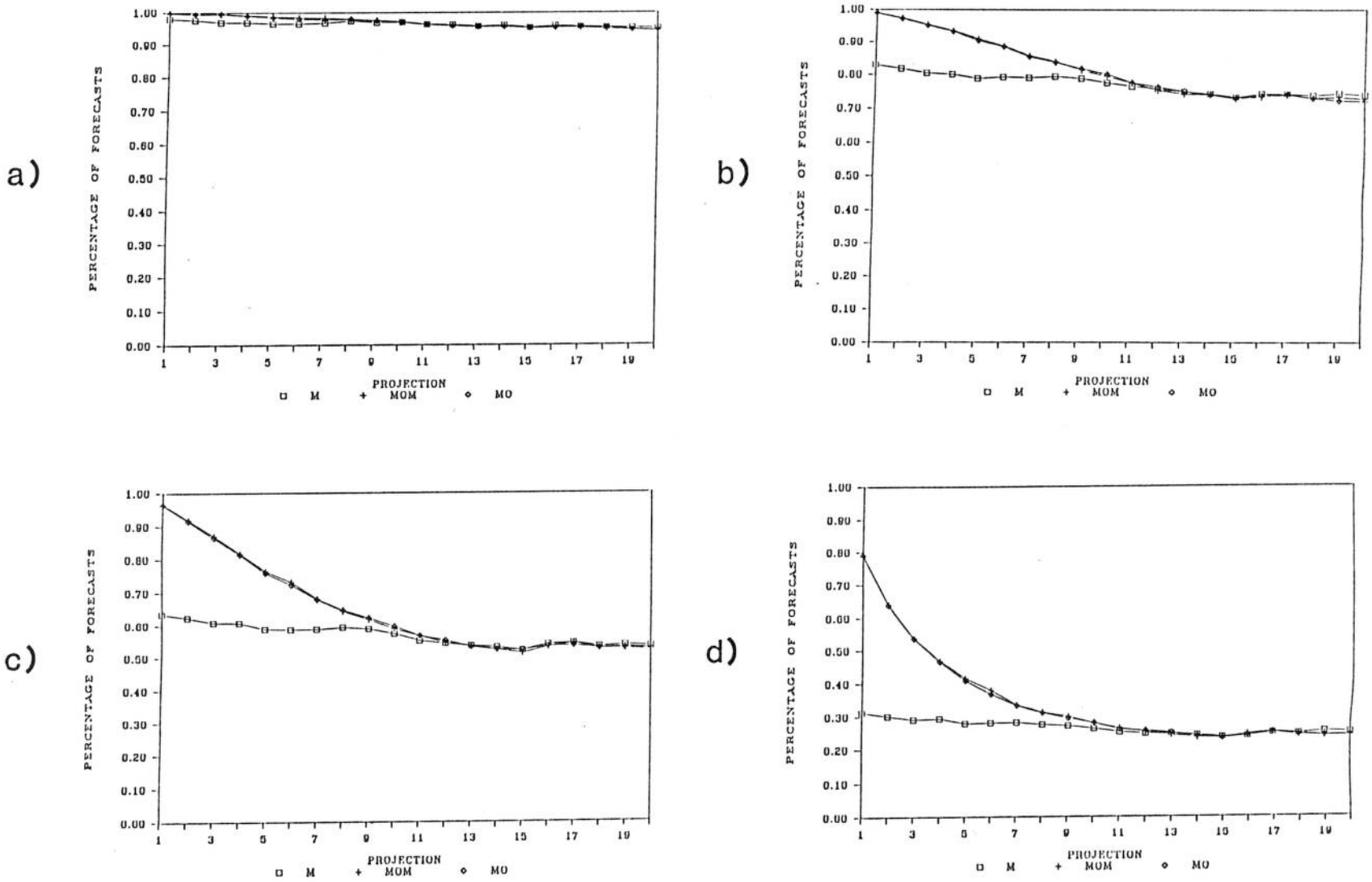

Figure 17. Percentage of hourly dew point forecasts within a) ± 10°F, b) ± 5°F, c) ± 3°F, and d) ± 1°F of the observed dew point by projection for M, MO, and MOM (MOS stations only).

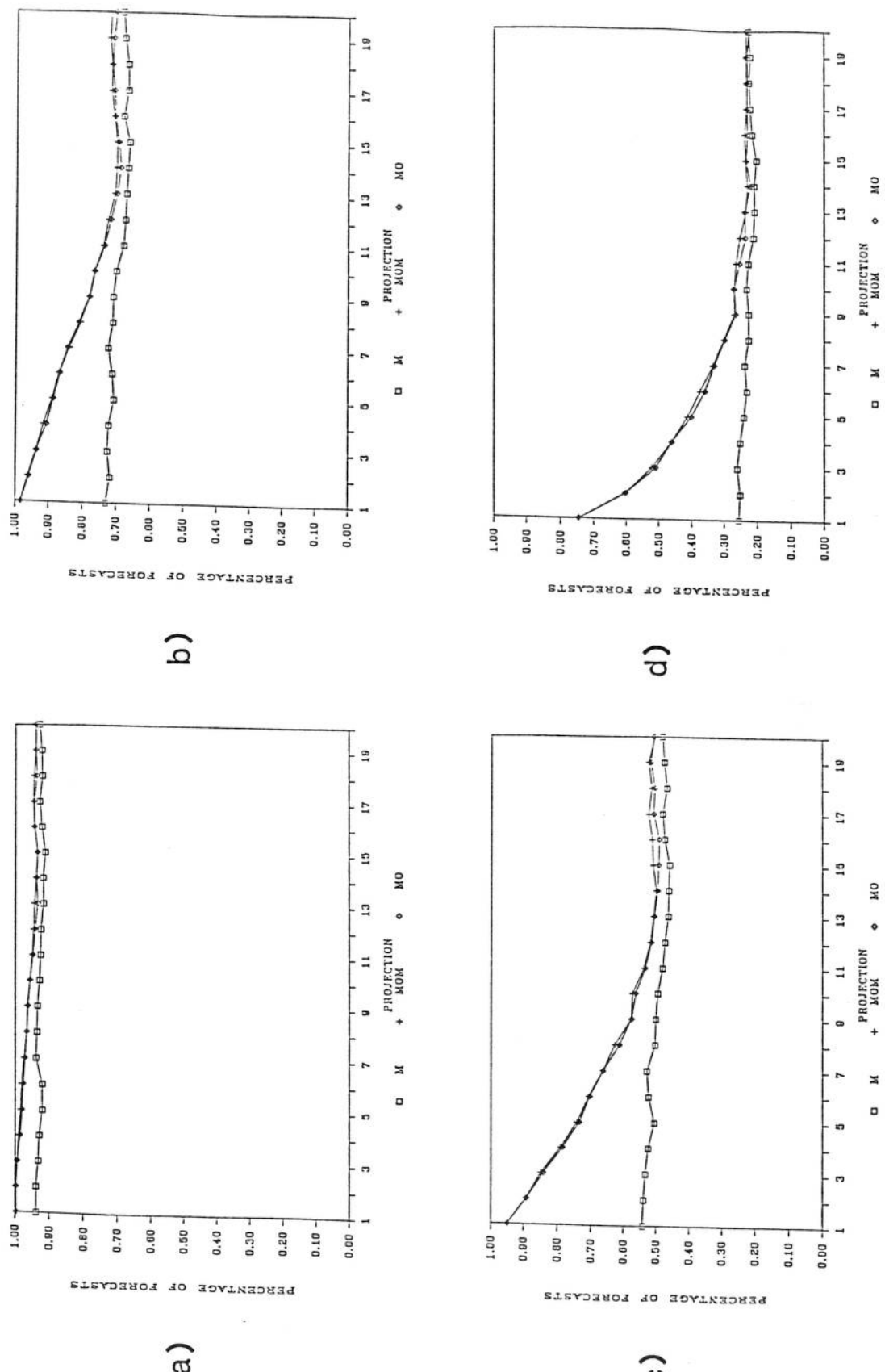

Figure 18. Same as Figure 17 but for non-MOS stations.

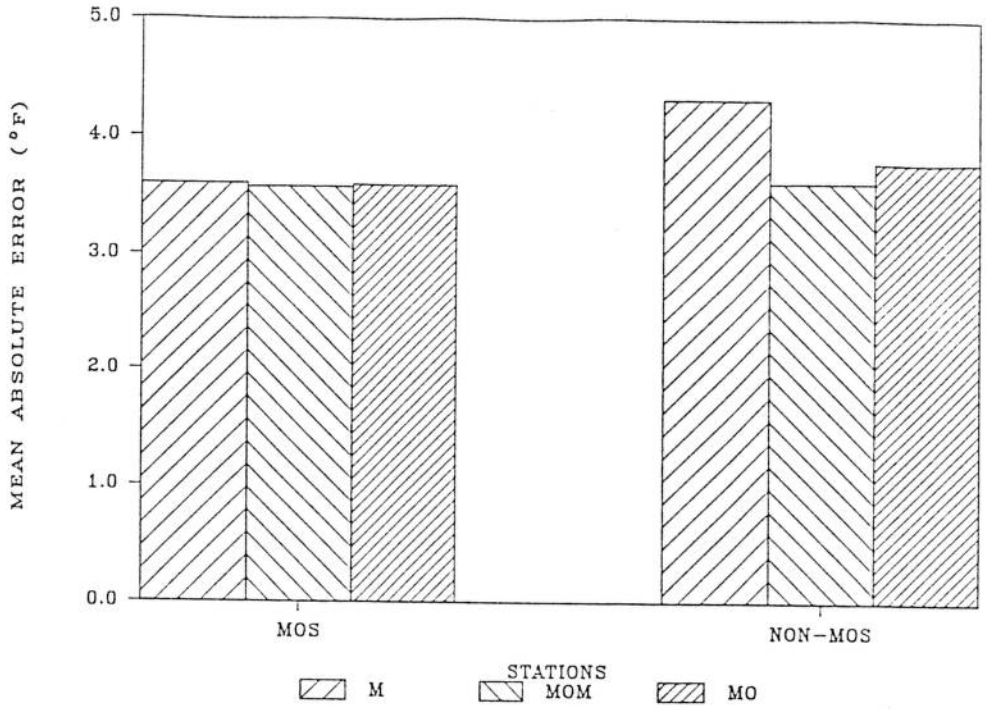

Figure 19. Mean absolute error of M, MOM, and MO maximum temperature forecasts (MOS and non-MOS stations).

APPENDIX I

Stations used in the study

The 103 stations from the MARD area used in this study are listed in Table 8.

Table 8. List of 103 stations included in the LAMP temperature, dewpoint, and maximum temperature study.

Call Letters	WBAN No.	Station Name	MOS Station
ABI	13962	Abiline, Tex.	X
ABQ	23050	Albuqerque, N. Mex.	X
ACT	13959	Waco, Tex.	X
AKO	24015	Akron, Colo.	
ALO	94910	Waterloo, Iowa	X
AMA	23047	Amarillo, Tex.	X
ATY	14946	Watertown, S. Dak.	
AUW	14897	Wausau, Wis.	X
BFF	24028	Scottsbluff, Nebr.	X
CDS	23007	Childress, Tex.	
CGI	3935	Cape Girardeau, Mo.	
CID	14990	Cedar Rapids, Iowa	
CNK	13984	Concordia, Kans.	X
CNM	93033	Carlsbad, N. Mex.	
CNU	13981	Chanute, Kans.	
COS	93037	Colorado Springs, Colo.	X
COU	3945	Columbia, Mo.	X
CPR	24089	Casper, Wyo.	X
CVS	22008	Cannon AFB, N. Mex.	
CYS	24018	Cheyenne, Wyo.	X
DAL	13960	Dallas, Tex.	
DDC	13985	Dodge City, Kans.	X
DEN	23062	Denver, Colo.	X
DFW	3927	Dallas-Ft. Worth, Tex.	X
DHT	93042	Dalhart, Tex.	
DMN	23078	Deming, N. Mex.	
DSM	14933	Des Moines, Iowa	X
DUG	93026	Douglass, Ariz.	
EAU	14991	Eau Claire, Wis.	X
EGE	23063	Eagle, Colo.	
ELD	93944	El Dorado, Ark.	
ELP	23044	El Paso, Tex.	X
FSD	14944	Sioux Falls, S. Dak.	X
FSM	13964	Fort Smith, Ark.	X
FYV	93993	Fayetteville, Ark.	
GAG	13975	Gage, Okla.	
GCK	23064	Garden City, Kans.	
GGG	3901	Longview, Tex.	
GJT	23066	Grand Junction, Colo.	X
GLD	23065	Goodland, Kans.	X
GRI	14935	Grand Island, Nebr.	X
GUP	23081	Gallup, N. Mex.	
GWO	13978	Greenwood, Kans.	X

Table 8. (Continued)

Call Letters	WBAN No.	Station Name	MOS Station
HMN	23002	Holloman AFB, N. Mex.	
HRO	13971	Harrison, Ark.	
ICT	3928	Wichita, Kans.	X
INK	23040	Wink, Tex.	
JAN	3940	Jackson, Miss.	X
JBR	1	Jonesboro, Ark.	X
JLN	13987	Joplin, Mo.	
LAR	24022	Laramie, Wyo.	
LBB	23042	Lubbock, Tex.	X
LBE	24023	North Platte, Nebr.	X
LFK	93987	Lufkin, Tex.	X
LHX	23067	La Junta, Colo.	
LIT	13963	Little Rock, Ark.	X
LND	24021	Lander, Wyo.	X
LNK	14939	Lincoln, Nebr.	X
LVS	23054	Las Vegas, N. Mex.	
MAF	23023	Midland, Tex.	X
MCB	93919	Mccomb, Miss.	X
MCI	3947	Kansas City, Mo.	X
MEM	13983	Memphis, Tenn.	X
MKC	13988	Kansas City Dwn, Mo.	X
MLC	93950	Mcalaster, Okla.	X
MLI	14923	Moline, Ill.	X
MLV	13942	Monroe, La.	
MSN	14837	Madison, Wis.	X
MSP	14922	Minneapolis, Minn.	X
NBE	93901	Dallas NAS, Tex.	
NQA	93839	Memphis NAS, Tenn.	
OFK	14941	Norfolk, Nebr.	X
OKC	13967	Oklahoma City, Okla.	X
OMA	14942	Omaha, Nebr.	X
OTM	14950	Ottumwa, Iowa	
PIA	14842	Peoria, Ill.	X
PIR	24025	Pierre, S. Dak.	X
PNC	13969	Ponca City, Okla.	
RAP	24090	Rapid City, S. Dak.	X
RFD	94822	Rockford, Ill.	X
RKS	24027	Rock Springs, Wyo.	X
ROW	23043	Roswell, N. Mex.	X
RST	14925	Rochester, Minn.	X
RWF	14922	Redwood Falls, Minn.	
RWL	24057	Rawlins, Wyo.	
SGF	13995	Springfield, Mo.	X

Table 8. (Continued)

Call Letters	WBAN No.	Station Name	MOS Station
SHR	24029	Sheridan, Wyo.	X
SHV	13957	Shreveport, La.	X
SJT	23034	San Angelo, Tex.	X
SLN	3919	Salina, Kans.	
SPI	93822	Springfield, Ill	X
SPS	13966	Sheppard AFB, Tex.	
STL	13994	St. Louis, Mo.	X
SUX	14943	Souix City, Iowa	X
TAD	23070	Trinidad, Co.	
TCC	23048	Tucumcari, N. Mex.	X
TOP	13996	Topeka, Kans.	X
TUL	13968	Tulsa, Okla.	X
TXK	13977	Texarkana, Ark.	X
TYR	13972	Tyler, Tex.	
VIN	93989	Quincy, Ill.	
VIH	13977	Vichy-Rolla, Mo.	
WRL	24062	Woorland, Wyo.	